



Full length article

The influence of spin in black hole triplets

A. Chitan ^{a,b,c}, , * A. Mylläri ^d, M. Valtonen ^{e,f,g}^a Physics and Astronomy department, University of Western Ontario, 1151 Richmond Street, London, N6A 3K7, Ontario, Canada^b Graduate Program in Astrophysics, Observatoire de Paris, Université PSL, CNRS, 5 pl. Jules Janssen, 92195, Meudon, France^c Physics department, University of the West Indies, Trinidad and Tobago^d Abo Akademi University, Turku/Abo, Finland^e Finnish Centre for Astronomy with ESO (FINCA), University of Turku, Turku, Finland^f Tuorla Observatory, Department of Physics and Astronomy, University of Turku, Turku, Finland^g Visitor, Institute of Astronomy, University of Cambridge, Madingley Road, Cambridge, England, United Kingdom

ARTICLE INFO

Dataset link: <https://doi.org/10.6084/m9.figshare.19735960.v2>, <http://www.astro.utu.fi/mikola/>, <https://doi.org/10.6084/m9.figshare.13194146.v1>

Keywords:
Black holes
Mergers
Dynamics
Spin

ABSTRACT

Spin can influence the dynamics of the already chaotic black hole triplet system. We follow this problem in two sets of simulations: first, the Agekian–Anosova region (or region D), and second, using Pythagorean triangles. We use ARCcode, an N-body code that performs numerical integration of orbits. This code includes post-Newtonian corrections, which we include up to the 2.5th order. In set one of our simulations, we fix the masses of the black holes at $10^6 M_{\odot}$. Then we run the simulations first without any spin added and after by initialising spin on one of the black holes. We find that after including spin into the system, 12.9% of the simulations changed outcomes. Either the systems went from having all black holes merging to having a black hole escaping the system, or vice versa. In the second set of simulations, we expanded into Pythagorean triangles as initial positions of black holes, stemming from Burrau's three-body problem. We varied the masses of the black holes from $10^0 M_{\odot}$ – $10^{12} M_{\odot}$. Black holes in these systems were given spin in normalised units ranging from 0 to ~ 0.95 . We find that intermediate mass black holes in the range of $10^4 M_{\odot}$ – $10^5 M_{\odot}$, were influenced the most by spin, particularly in their lifetimes. We also find that simulations, initialised as 2-dimensional, become 3-dimensional.

1. Introduction

The detection of black hole mergers is becoming more and more commonplace in modern astrophysics, because of the advanced Laser Interferometer Gravitational-Wave Observatory (LIGO) and the European gravitational wave observatory systems (Abbott et al., 2019, 2021). The mergers of stellar mass black holes (SBH) have dominated earth-based detections, but it is expected that, with space-based detectors like the Laser Interferometer Space Antenna (LISA), finding mergers of intermediate mass black holes (IMBH) as well as supermassive black holes (SMBH) could be possible (Rhook and Wyithe, 2005). One theory of the origin of these mergers is via isolated binaries (McMillan and Portegies Zwart, 2001; Belczynski et al., 2002). However, a triplet origin (a system of three black holes) is also a viable theory, as two black holes can merge due to the gravitational influence of the third (Rodríguez and Antonini, 2018). Triplet SBH systems can form from isolated triplet star systems (Vigna-Gómez et al., 2021). IMBHs have, so far, been hard to detect, but recent advances have been made by Peiřker et al. (2024). Triplet IMBH systems can form

within globular clusters (Sigurdsson and Hernquist, 1993; Vitral and Mamon, 2021), and the hierarchical merging of galaxies can potentially lead to the formation of triplet SMBHs (Valtonen, 1996; Hoffman and Loeb, 2007; Kollatschny et al., 2020; Yadav et al., 2021), since most massive galaxies host a SMBH at their core (Kormendy and Richstone, 1995). With such rapid advancements in the field of gravitational wave physics, the study of the dynamics of triplet black hole systems is necessitated.

But triplet systems, and the wider three-body, are complex and chaotic. Recent strides have been made to develop a solution to the three-body problem, both analytically (Heggie and Rasio, 1996; Stone and Leigh, 2019; Hamers and Samsing, 2019; Ginat and Perets, 2021), and numerically (Szebehely and Peters, 1967; Monaghan, 1976; Hut and Bahcall, 1983; Hut, 1983, 1993; Heggie and Hut, 1993; Goodman and Hut, 1993; McMillan and Hut, 1996; Heggie et al., 1996). We are interested in the configurations proposed by Burrau (1913), known as Burrau's problem of three bodies. This problem, though popularised by Burrau, was initially brought to his attention by Ernst Meissel (Peetre,

* Corresponding author at: Physics and Astronomy department, University of Western Ontario, 1151 Richmond Street, London, N6A 3K7, Ontario, Canada.
E-mail address: achitan2@uwo.ca (A. Chitan).

1995; Valtonen et al., 2016a). In this problem he describes three bodies placed at the vertices of a 3,4,5 Pythagorean triangle with masses reflecting the side of the triangle opposite to each body. Meissel believed the problem to have a periodic solution while Burrau was unable to find, more rigorously, any proof of this. The evolution of such a system was later studied extensively by both Szebehely and Peters (1967) and Valtonen et al. (1995). In the work of the former, they integrated the orbital motion computationally and found that eventually such a triplet system would end in a bound binary and an escaping body. Valtonen et al. studied, from a relativistic approach, the influence of mass variation from $10^5 M_{\odot}$ to $10^9 M_{\odot}$ in five different cases. They found that for smaller mass systems, binary formation and escape was how the system would typically end, but for larger masses, mergers would take place instead.

In Chitan et al. (2021), some of the authors re-analysed this work and extended the mass ranges from $10^0 M_{\odot}$ to $10^{12} M_{\odot}$ for initial configurations of all Pythagorean triangles with hypotenuse <100 pc. It was found that as the mass increased, the fraction of mergers also increased and the lifetimes of the triplet systems decayed exponentially. Distinctions were also made between triangles that were close to a hierarchical configuration and those that were not, using the definitions proposed by Anosova et al. (1990). Here hierarchical triangles are the triangles where there a distinctive inner binary and a third body orbiting from far away is obvious. For non-hierarchical triangles, this distinction is less obvious. In the more hierarchical type triangles in the study, merging dominated even from low mass black holes ($10^0 M_{\odot}$ – $10^3 M_{\odot}$) and their evolution was more predictable than that of the more non-hierarchical triangles. The more non-hierarchical triangles, like the 3,4,5, exhibited a more chaotic nature. We also saw that there was a transition from escape dominated dynamics to merger dominated dynamics in such triplet systems as was shown by Valtonen et al. (1995). Boekholt et al. (2021) also studied the same 3,4,5 Pythagorean configuration using the code BRUTUS with 2.5th order post-Newtonian (pN) terms and 1pN cross terms. They also replicated the transition from escapes to mergers in such triplet systems.

All black holes in the triplet systems studied were kept as non-rotating in Chitan et al. (2021). But, we expect black holes to rotate. Kerr (1963) studied mathematically this more realistic case of rotating black holes. Following the no-hair theorem, a fully isolated black hole can be described by only three parameters — its mass, M , its spin, J (Israel, 1967, 1968; Hawking, 1972), and its charge (which we do not consider here). We take the next step here, in this paper, by including an analysis of the effect of spin in black hole triplets.

As gravitational wave physics and the study of black holes become more prominent in modern astrophysics, it is important to consider what the effect of spin will have on black hole dynamics. Idealised Schwarzschild black holes are much ‘easier’ to deal with than their much more realistic Kerr counterparts. However, almost all astrophysical bodies do rotate and the relativistic effects associated may have an impact on the evolution of n-body systems. One of the major effects of having a rotating black hole in the system is relativistic frame-dragging. The spacetime around the rotating black hole would be dragged and therefore affect other orbiting bodies (in this case the other two black holes of our triplet system). From this comes the Lense-Thirring effect whereby the argument of periastris as well as the longitude of the ascending node precesses due to the frame-dragging effect of a rotating body in the system (Lense and Thirring, 1918; Ciufolini and Pavlis, 2004).

Fang et al. in a series of papers looked at hierarchical triplet systems with a rotating SMBH and inner binary comprised of SBHs (Fang and Huang, 2019; Fang et al., 2019; Fang and Huang, 2020). The typical von Zeipel–Kozai–Lidov oscillations imposed in such systems are with respect to non-rotating bodies. Fang et al. compared the evolution of triplet systems in the hierarchical formation with and without SMBH spin in order to compare the effect of the von Zeipel–Kozai–Lidov oscillations to other effects that may be introduced due to the spin of

the SMBH. They found that there were significant differences in the evolution of the inner binary black hole system when spin was included — depending on the initial orbital angles, the merger time of the binary could be lengthened or shortened if spin was present (Fang et al., 2019). They also conducted numerical simulations to show that the effect of spin could be detectable by the upcoming LISA. This could potentially lead to new ways of observing the spin effect in triplet systems as well as the spin parameters of SMBHs (Fang and Huang, 2020).

Kidder (1995) discusses in depth the effect of spin on a coalescing binary in the pN regime. They show that one of the major contributions of these spin terms to the orbital dynamics is that they are not confined to the orbital plane. They then result in the precession of the orbital plane if the spin vector is not aligned perpendicular to the orbital plane. They also demonstrate the spin contribution to energy loss as well as the angular momentum loss in gravitational radiation, where they show that the spin-orbit contribution can be significant. The role of spin in the evolution of such systems can be expected to have a significant effect. This provides the motivation to test this effect via numerical simulations on not binaries but on the more complex but also astrophysically common triplet systems.

In this paper, we extend the work of Chitan et al. (2021) by allowing the most massive black hole in the triplet system to rotate and conducting numerical simulations using ARCCode. The spin vector as well as the masses of the black holes are varied. This is presented in the following sections — in Section 2 we will focus on the method and dataset. In Section 3, the results for the effect of increasing spin vector and increasing mass will be presented and discussed.

2. Setup

The units that we use are astronomical units (AU) for distance ($\sim 1.5 \times 10^{11}$ km), solar masses (M_{\odot}) for mass ($\sim 2 \times 10^{30}$ kg) and years (yr) for time ($\sim 3 \times 10^7$ s). One astronomical unit is the distance between the Earth and the Sun and a solar mass is the mass of our Sun. In some cases we use time in terms of crossing time of a system where the crossing time is given by Eq. (1) (Valtonen and Karttunen, 2006). Here G is the gravitational constant, M is the total mass of the system and E_0 is the energy of the system.

$$T_{cr} = GM^{5/2}(2|E_0|)^{-3/2} \quad (1)$$

ARCCode was provided by Prof. Seppo Mikkola (Mikkola and Aarseth, 1993, 1996; Mikkola and Tanikawa, 1999; Mikkola and Aarseth, 2002; Mikkola and Merritt, 2006, 2008; Hellström and Mikkola, 2010; Mikkola and Tanikawa, 2013a,b) where we used up to 2.5th order pN corrections for 3-body simulations. The spin-orbit terms (which are presented at the 1.5 pN order (Barker and O’Connell, 1975)) used in the numerical integration are explained in detail by Valtonen et al. (2010) and by Mikkola (2020a). This is summarised briefly in 2.1.

2.1. Code implementation

ARCCode conducts orbital numerical integration of the system of triplets based on initial conditions placed by the user. For this work we conduct simulations with post-Newtonian corrections up to the 2.5th order.

This code performs orbital integration using a logarithmic Hamiltonian leapfrog method. The transformed equations of motion for both the time and co-ordinates are obtained from the logarithmic Hamiltonian (a full derivation is presented in Mikkola and Tanikawa (2013b)). Using the leapfrog algorithmic method, these equations can be solved approximately.

The pN equations developed by Mora and Will (2004) and further explained in Mikkola (2020b) which are used for integration (up to the 2.5th order) are listed here. Here, we consider two bodies m_1 and m_2

with separation, r and relative velocity, v , where $m = m_1 + m_2$; $\eta = \frac{m_1 m_2}{m^2}$ and $\mathbf{n} = \frac{\mathbf{r}}{r}$.

The pN equations used, up to 2.5th order, are as follows:

$$A_1 = 2(2 + \eta) \left(\frac{m}{r}\right) - (1 + 3\eta) v^2 + 1.5\eta \dot{r}^2 \quad (2)$$

$$A_2 = -\frac{3}{4} (12 + 29\eta) \left(\frac{m}{r}\right)^2 - \eta (3 - 4\eta) v^4 + (2 + 25\eta + 2\eta^2) \left(\frac{m}{r}\right) \dot{r}^2 + 1.5\eta (3 - 4\eta) v^2 \dot{r}^2 \quad (3)$$

$$A_{2.5} = \frac{8}{5} \eta \frac{m}{r} \dot{r} \left(\frac{17}{3} \frac{m}{r} + 3v^2\right) \quad (4)$$

$$B_1 = 2(2 - \eta) \dot{r} \quad (5)$$

$$B_2 = -\frac{1}{2} \dot{r} [(4 + 41\eta + 8\eta^2) \left(\frac{m}{r}\right) - \eta (15 + 4\eta) v^2 + 3\eta (3 + 2\eta) \dot{r}^2] \quad (6)$$

$$B_{2.5} = -\frac{8}{5} \eta \left(\frac{m}{r}\right) \left[3 \left(\frac{m}{r}\right) + v^2\right] \quad (7)$$

Then, the total effect on the acceleration of the bodies is given by the following:

$$A_{tot} = A_1/c^2 + A_2/c^4 + A_{2.5}/c^5 \quad (8)$$

$$B_{tot} = B_1/c^2 + B_2/c^4 + B_{2.5}/c^5 \quad (9)$$

Which is then written in the acceleration term as:

$$\ddot{\mathbf{r}} = \ddot{\mathbf{r}}_N - \frac{m}{r^2} (A_{tot} \mathbf{n} + B_{tot} \mathbf{v}) + \ddot{\mathbf{x}}_{SO} + \mathbf{x}_Q \quad (10)$$

The term, $\ddot{\mathbf{x}}_{SO}$ is the spin-orbit contribution and \mathbf{x}_Q is the quad rupole-monopole term. Both describe the effect of spin on the acceleration of the body. From [Barker and O'Connell \(1975\)](#) and described in [Valtonen et al. \(2010\)](#) these terms are defined as follows:

$$\ddot{\mathbf{x}}_{SO} = \frac{Gm}{r^2} \left(\frac{Gm}{c^3 r}\right) \left(\frac{1 + \sqrt{1 - 4\eta}}{4}\right) \times \chi \left[(12 [s_1 \cdot (\mathbf{n} \times \mathbf{v})]) \mathbf{n} + \left[(9 + 3\sqrt{1 - 4\eta}) \dot{r} \right] (\mathbf{n} \times s_1) - \left[7 + \sqrt{1 - 4\eta} \right] (\mathbf{v} \times s_1) \right] \quad (11)$$

$$\ddot{\mathbf{x}}_Q = \chi^2 \frac{3G^3 m_1^2 m}{2c^4 r^4} [(5(\mathbf{n} \cdot s_1)^2 - 1) \mathbf{n} - 2(\mathbf{n} \cdot s_1) s_1] \quad (12)$$

In the spin-orbit and quadrupole-monopole terms, χ represents the spin parameter and s_1 represents the spin of the black hole.

2.1.1. Constraints

ARCcode does not use cross terms which over relativistic timescales become necessary for describing the evolution of systems ([Will, 2014a,b](#)). However, for this study our aim is to see via the use of ARCcode, if there is any measurable effect of the inclusion of spin. Here, we focus on studying the influence of spin on the final outcomes of the triplets statistically.

We also limit the case to where only one of the black holes in our triplet system has spin. This is because ARCcode allows only one of the black holes to rotate within a given simulation. However, in numerical integration, if one black hole is much bigger than the others, then the spin of the smaller black hole is considered negligible ([Mikkola, 2020b](#)). In our simulations, though the masses are on similar scales we always choose the largest black hole to be the rotating one of the three.

2.2. Initial conditions

All black holes begin with zero initial velocity and only one of them is allowed to rotate — this is the biggest black hole in each triplet system. The magnitude of the spin vector is kept to <1 in normalised units as a spin magnitude $=1$ results in zero surface gravity of the black hole and the theoretical naked singularity which theoretically cannot exist ([Bardeen et al., 1973](#); [Wald, 1999](#)). All bodies start with co-ordinates limited to the xy-plane. Timescales were kept as in [Chitan et al. \(2021\)](#), with the crossing times of systems being utilised for

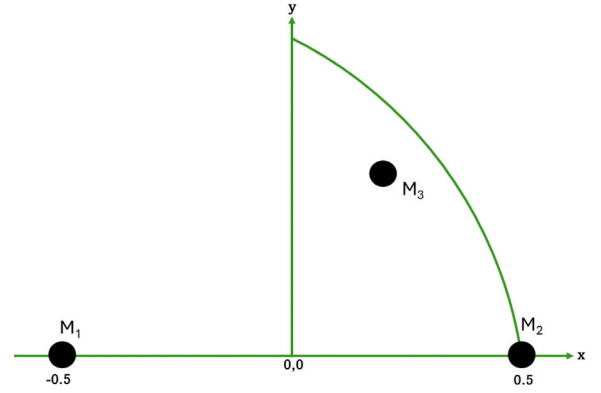


Fig. 1. A sketch of the initial placements of black holes in the Agekian-Anosova homology region (region D). Black holes M_1 and M_2 are fixed on the negative and positive x -axis respectively, while black hole M_3 , varies within the bounded region (x -axis, y -axis and circle arc), making up the unique simulations. This describes phase space for the zero initial velocity, equal mass three body system. This was used for the setup of simulations of set one of our study.

comparisons of lifetimes.

We focus first on the Agekian-Anosova homology region, also referred to as region D. This forms *set one* of our simulations. This region describes the phase space region for zero initial velocity, equal mass three body systems ([Anosova and Orlov, 1984](#); [Anosova and Nebukin, 1991](#); [Anosova et al., 1994](#)). In this space, two bodies are fixed at coordinates $(0.5, 0)$ and $(-0.5, 0)$ while the third body is placed in the region within the unit circle centered at $(-0.5, 0)$ and bounded by the x and y axes. This is shown in [Fig. 1](#). By varying the position of M_3 within this bounded region, a complete run of simulations is made. The bounded region was sampled by constructing 1000 circles centered at $(-0.5, 0)$ with decreasing radii. The upper limit for the radii was that of the initial unit circle and the lower limit was 0. Only quadrant one ($x > 0, y > 0$) was considered. Each of these circle arcs were constructed of individual points with an angular stepsize of 0.01. These points for all of the circles created the set of positions in which the M_3 body was placed during simulations. For each run, there were 8094 different positions of M_3 , making 8094 individual simulations per run.

In *set one*, we run simulations with all Schwarzschild black holes. Then, we re-run the simulations with a black hole M_3 , having a spin magnitude near unity (~ 0.95 , with spin orientation $[0.55 \ 0.55 \ 0.55]$). The spin magnitude was kept along the diagonal for simplicity and not to introduce extra variability in an already complex system. We also wanted to observe motion of our system in 3-dimensions therefore our spin values are not aligned in any one plane. To fully cover the geometrical Agekian-Anosova region we also repeated simulations with M_3 fixed at $(-0.5, 0)$ and then fixed at $(0.5, 0)$. A summary of this is provided in [Table 1](#). The results of the last two runs are provided in the Appendix.

Set two of our simulations come from the Pythagorean triangles and Burrau's problem. We conducted in-depth simulations including both increasing spin and increasing mass (See [Table 2](#) for list of triangles and [Table 3](#) for spin and mass setups). The typical 3,4,5 triangle is provided in 3,4,5. The black holes are initialised such that their masses are multiples of the side of the triangle they are opposite from. When we configure the triangles, the masses of the black holes that we are studying are multiplied by the value given by the particular triangle. The most massive black hole is the one that spin is added to. The distances, shown as 'd' in [Fig. 2](#), were kept at 206265 AU in our simulations. This value is equivalent to 1 parsec.

In our previous study ([Chitan et al., 2021](#)) we used an informal method of classifying the triangles into either more hierarchical, or less

Table 1

A summary of set one simulations. Following the setup shown in Fig. 1. Each Run consists of 8094 individual simulations where M_1 and M_2 stay fixed on the negative and positive x-axis, respectively, but M_3 moves each time within the bounded region. An initial run was conducted where none of the black holes had spin, as a control. To cover the Agekian–Anosova region fully, we also conduct runs three and four where the spinning black hole is fixed at M_1 and M_3 , respectively. Black hole mass is fixed at $10^6 M_\odot$, with the spinning black hole being more massive at $10^7 M_\odot$ for each case.

Run	Black Hole Position	Spin Vector	Mass ($10^6 M_\odot$)	(x,y) Position
One	M_1	[0 0 0]	1	(-0.5,0)
	M_2	[0 0 0]	1	(0.5,0)
	M_3	[0 0 0]	10	varying within region D
Two	M_1	[0 0 0]	1	(-0.5,0)
	M_2	[0 0 0]	1	(0.5,0)
	M_3	[0.55 0.55 0.55]	10	varying within region D
Three	M_1	[0.55 0.55 0.55]	10	(-0.5,0)
	M_2	[0 0 0]	1	(0.5,0)
	M_3	[0 0 0]	1	varying within region D
Four	M_1	[0 0 0]	1	(-0.5,0)
	M_2	[0.55 0.55 0.55]	10	(0.5,0)
	M_3	[0 0 0]	1	varying within region D

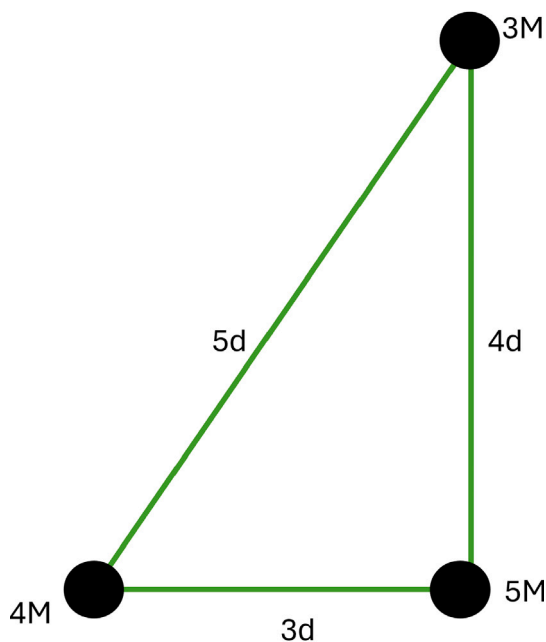


Fig. 2. A sketch of the 3,4,5 triangle, one of the Pythagorean triangles used for the initialisation of set two simulations. The placement of the black holes are represented by the black dots at the vertices of the triangle. The mass of each black hole is multiplied by the length of the side of the triangle opposite to it.

hierarchical, depending on the angle between the hypotenuse and the second longest side of the triangle. If there was an angle $> 30^\circ$, the triangle was considered a non-hierarchical triangle and if the angle was $< 30^\circ$, a hierarchical triangle. This is shown in Table 2.

The effect of increasing spin was the focus for set two. We were interested in seeing how the effect of spin varied across the different masses of the black holes, shown in Table 3. For these simulations, we increased the masses of the black holes from $10^0 M_\odot$ to $10^{12} M_\odot$ in increasing factors of 10. The intermediate mass range of $10^4 M_\odot$ to $10^7 M_\odot$ was especially interesting since this is where most variability in the outcomes of our systems might be expected. Because of this we conducted ‘zoomed’ in simulations of this region, by increasing the mass not by factors of $10^1 M_\odot$, but, by factors of $10^{0.2} M_\odot$. Furthermore, from our first study of the Pythagorean setup in Chitan et al. (2021),

Table 2

A list of the Pythagorean triangles used for set two of this study. We classify them into hierarchical or non-hierarchical based on the angle between the hypotenuse and the second longest side of the triangle. If the angle is $< 30^\circ$, it is considered hierarchical.

Triangle	Classification	Angle ($^\circ$)
3,4,5	Non-Hierarchical	36.87
5,12,13	Hierarchical	22.62
7,24,25	Hierarchical	16.26
8,15,17	Hierarchical	28.07
9,40,41	Hierarchical	12.68
11,60,61	Hierarchical	10.39
12,35,37	Hierarchical	18.93
13,84,85	Hierarchical	8.80
16,63,65	Hierarchical	14.25
20,21,29	Non-Hierarchical	43.60
28,45,53	Non-Hierarchical	31.89
33,56,65	Non-Hierarchical	30.51
36,77,85	Hierarchical	28.07
39,80,89	Hierarchical	28.07
48,55,73	Non-Hierarchical	41.11
65,72,97	Non-Hierarchical	42.08

Table 3

A summary of set two simulations for the Pythagorean triangles. For these simulations, the masses of the black holes as well as the spin magnitude are increased for each of the Pythagorean triangle setups we used.

$\log_{10}(\text{Mass } (M_\odot))$	Spin Vector
0, 1, 2, 3, 4, 4.2, 4.4,	[0 0 0], [0.05 0.05 0.05], [0.1, 0.1, 0.1], [0.15,
4.6, 4.8, 5, 5.2, 5.4, 5.5,	0.15, 0.15], [0.2, 0.2, 0.2], [0.25, 0.25, 0.25],
5.6, 5.8, 6, 6.2, 6.4, 6.6,	[0.3, 0.3, 0.3], [0.35, 0.35, 0.35], [0.4, 0.4, 0.4],
6.8, 7, 8, 9, 10, 11	[0.45, 0.45, 0.45] [0.5, 0.5, 0.5], [0.55 0.55 0.55]

the mass of $10^{5.5} M_\odot$, was where we found that triplets switched from escape dominated dynamics to merger dominated dynamics, so we also conducted extra simulations for this specific mass.

In the first of run of set two simulations, we increased the mass of the black holes from $10^0 M_\odot$ to $10^{12} M_\odot$ in increasing factors of 10. For the second run we zoomed in more closely to the mass range of $10^4 M_\odot$ to $10^7 M_\odot$ in increasing factors of $10^{0.2} M_\odot$. For the third run we focused only on the $10^{5.5} M_\odot$ mass since this mass was found to be the mass of our black hole triplets at which triplets preferred a merger outcome to an escape outcome (Chitan et al., 2021). For each of these simulations, the most massive of the black holes was the one given an initial spin. This spin varied from [0,0,0] to [0.55,0.55,0.55] increasing with [0.05,0.05,0.05]. As with set one, spin magnitudes were kept along the diagonal for simplicity and to observe 3-dimensional motion. The summary of the set two simulations is given in Table 3.

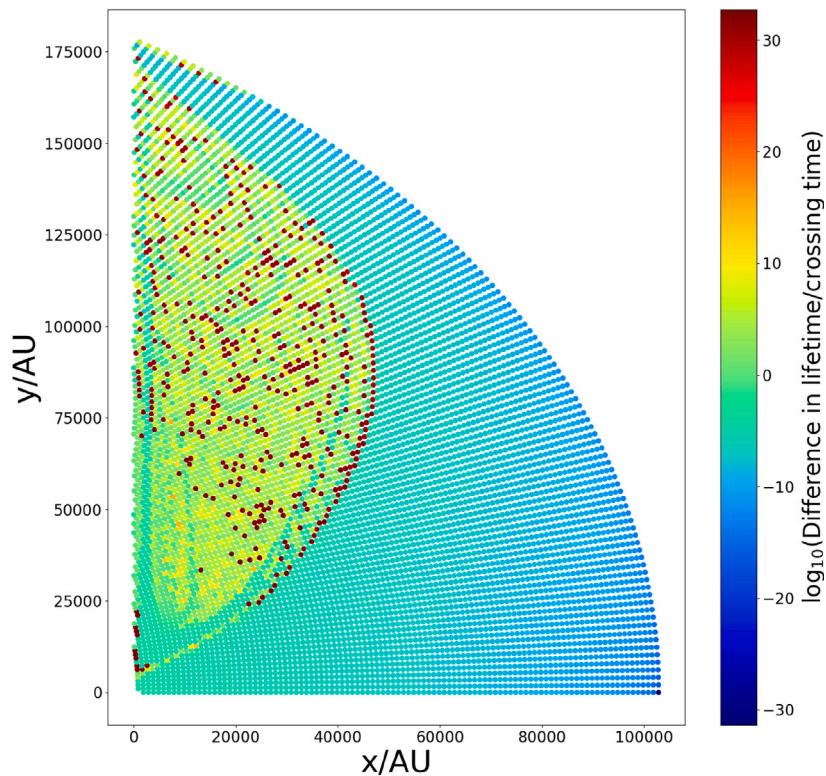


Fig. 3. A colour plot showing the difference in lifetime between simulations with spin and simulations with no spin for our set one simulations. The individual dots represent the initialisation of each individual simulation, while the colour shows the magnitude of difference in $\log_{10}(\text{lifetime}/\text{crossing time})$ between spin and no spin cases. Here the masses of the fixed black holes are $10^6 M_{\odot}$. The spinning black hole varies within the region D in every simulation and has a mass of $10 \times 10^6 M_{\odot}$.

3. Results

3.1. The effect of spin in set one

For set one of our simulations, we made use of the Agekian–Anosova region. This was summarised in Table 1. This setup involved fixing two of our black holes on the x -axis and varying the position of the third black hole within the bounded region shown in Fig. 1. The two main scenarios we focus on here are: 1. when the most massive black hole spins and 2. when none of our black holes have spin. These correspond to Run One and Run Two in Table 1.

The first thing that we notice are the lifetimes of our systems, i.e. how long does it take a triplet to become just a binary? This happens either when two black holes merge or when one black hole escapes. We find that there are some noticeable changes in the lifetimes with the addition of spin. This is shown by the colour plot of Fig. 3. This figure plots each initial setup; each point represents where the spinning black hole started off within the bounded region of the Agekian–Anosova mapping. The colour of the points refers to how big of a difference there is in lifetime between the spin and no spin runs. There appears to be a more well-defined region (the green portion) which feels the influence of spin more strongly than the outer portion. The red dots show that, in some cases, the inclusion of spin changes the lifetime of the system by 30 orders of magnitude. The three-body problem is inherently chaotic. A small change in initial conditions can result in a large change in the final outcome. This is what we see here in some of our simulations. The green portion of the plot describes more non-hierarchical setups which are known to be even more unpredictable than the hierarchical ones.

Another parameter we consider is how exactly the triplet ends its lifetime. This happens when wither two of the three black holes merge or when one of the black holes, after a close encounter, escapes from the center of mass of the system. The former case, we refer to as a merger, and the latter, we refer to as an escape. Since the spin can

have an influence on the lifetimes of our systems, as discussed above, it can potentially have an influence on the final outcomes of the triplets too. We look at the ‘change in outcome’ of our triplets in Fig. 4. We see that in 12.9% of our triplets of set one, the final outcome of the triplet changes when spin is added. This means that if previously the triplet ended via merger, with the addition of spin it ended via escape instead.

3.2. The effect of increasing spin in set two

We then looked at the Pythagorean triangular configurations for our set two simulations. This was summarised in Table 3. Unlike set one, in set two we also varied the masses of our black holes. The masses ranged from $10^0 M_{\odot}$ – $10^{12} M_{\odot}$. Here, we take a look at the changes in lifetimes of the systems as we did above with the set one simulations. Since we found that above the mass $10^8 M_{\odot}$, there was no discernible effect of spin, we focus more on the intermediate mass range. It is at these masses that we observe some variation in the lifetimes of the systems that can be attributable to spin. This is shown in Fig. 5, the zoomed in set of simulations of our intermediary masses. Spin has a small but noticeable effect on the lifetimes around the $10^4 M_{\odot}$ – $10^5 M_{\odot}$ mass range, with triplets of mass $10^{4.4} M_{\odot}$ appearing to have been affected the most.

We then focused on two specific masses: $10^{4.4} M_{\odot}$ and $10^{5.5} M_{\odot}$. At $10^{4.4} M_{\odot}$, we observed the most noticeable effect of spin on triplet lifetimes and at $10^{5.5} M_{\odot}$, we expect to be a transitory mass from escape dominated dynamics to merger dominated dynamics.

For each of the 16 triangular configurations, two mergers are possible allowing 32 total merger events possible per black hole spin value that we simulated. The number of mergers occurring at each spin value, in increasing spin magnitude, is shown in Fig. 6. Across all spin magnitudes, the number of mergers stays around 14 (i.e. approximately 40% of the 32 possible mergers occur) for the $10^{5.5} M_{\odot}$ mass. From our previous study with no spin, at $10^{5.5} M_{\odot}$, this was slightly higher with ~

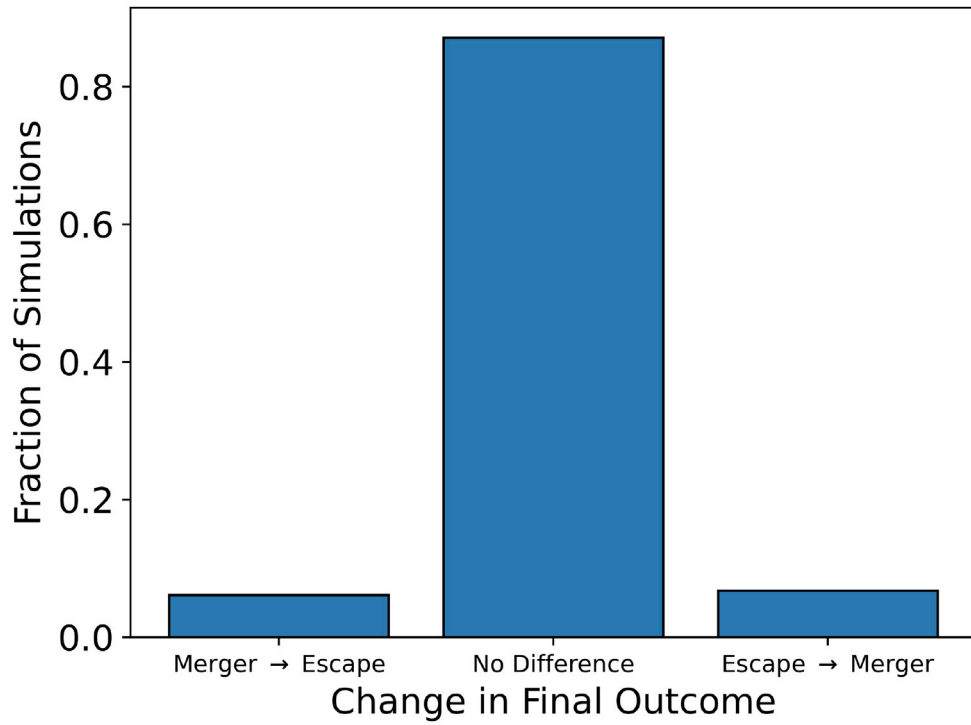


Fig. 4. A bar chart showing the fraction of simulations that experience a difference (or no difference) in final outcome when one of the black holes is given a spin in our simulations from set one. Merger means the system ends when two black holes have merged, escape means that one of the black holes escapes the triplet center of mass.

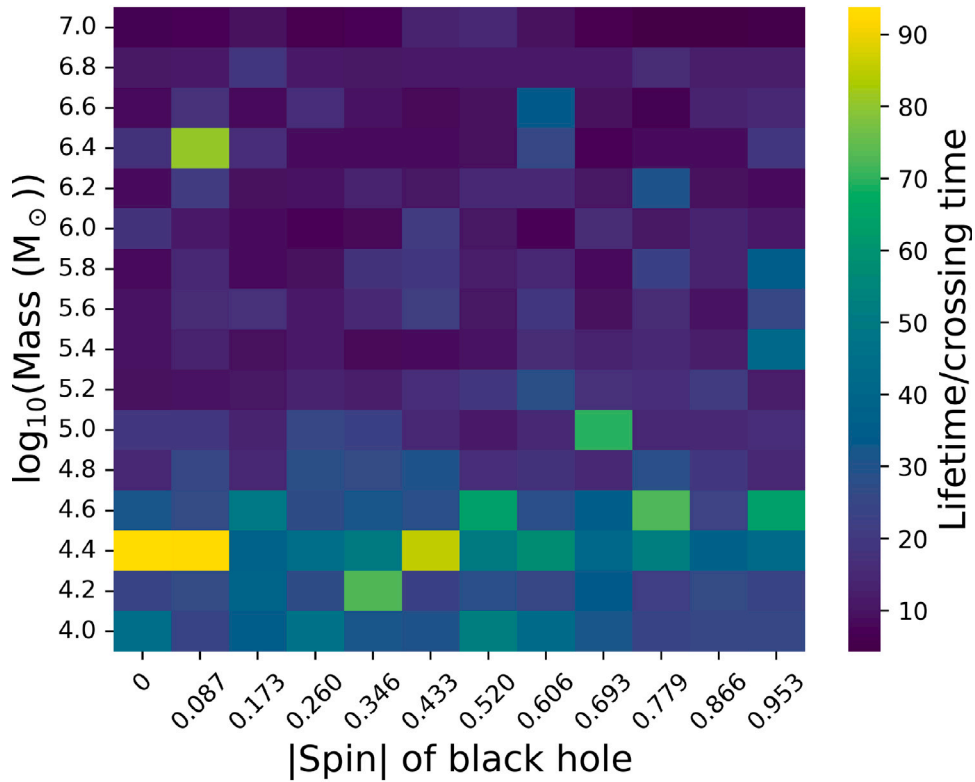


Fig. 5. A colour plot showing the average lifetime, in crossing time, for all the Pythagorean triangles of set two within the mass range of $10^4 M_{\odot}$ – $10^7 M_{\odot}$ and with increasing spin magnitude.

50% of possible mergers occurring. While the difference is very subtle, it may be that adding spin helps to facilitate escape over merger. At the mass of $10^{4.4} M_{\odot}$, triplets are a bit more stable in terms of mergers as spin increases. While the final outcome itself does not change too much,

the overall lifetimes still are affected as was previously discussed. We do note that there is a slightly higher number of mergers (7) in the no spin case, compared to the spin cases. However, this can again be a sign of chaos.

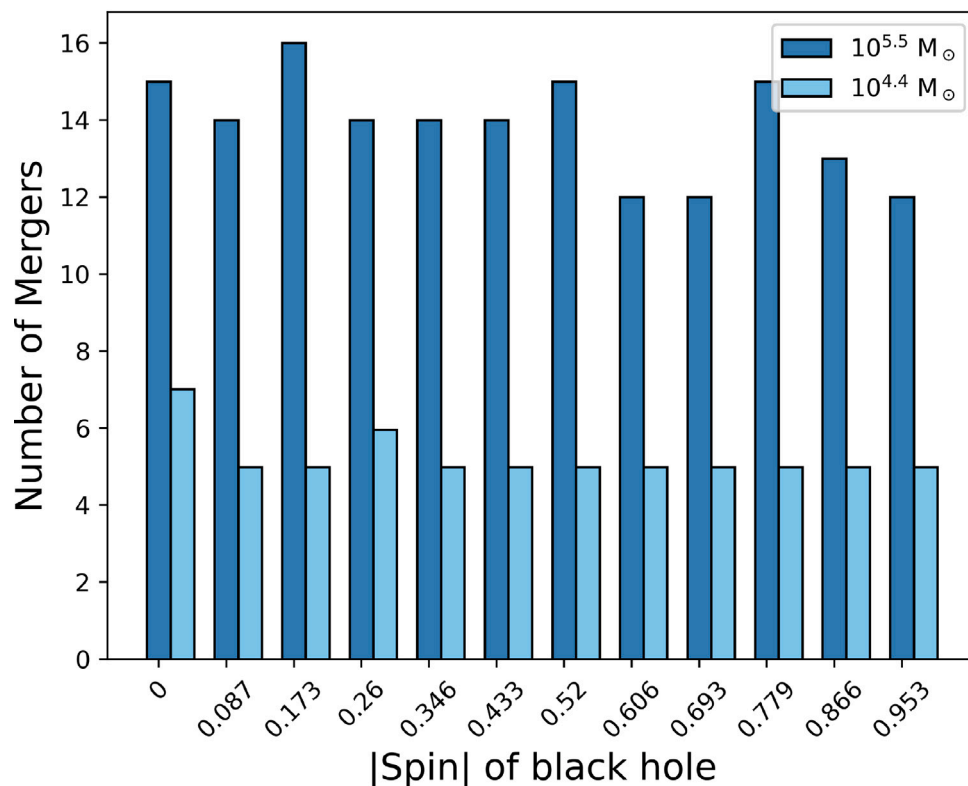


Fig. 6. The fraction of mergers that take place among all the triangles of set two simulations at $10^{4.4} M_{\odot}$ and $10^{5.5} M_{\odot}$ vs. increasing spin magnitude of the most massive black hole in each system. At each spin magnitude a total of 32 mergers is possible since we have 16 initial triangles and 2 possible mergers per triangle setup.

The next defining parameter that we chose to analyse was the 3-dimensional motion of our triplets. Spin can naturally transform the 2-dimensional motion of a system into 3-dimensional. For our triplets, all black holes are initialised within the x-y plane. The spin that we add, however, is 3-dimensional. The magnitude of change from 2-dimensional motion to 3-dimensional motion can be used as a measure of how influential spin is. We do this by finding the maximum z coordinate achieved by the spinning black hole while the triplet is intact i.e. before there is a merger or an escape. We normalise this z value to the hypotenuse of each triangle and find the average maximum z-coordinate among all triangles at each spin value we simulated. We show this in Fig. 7. This colour plot has spin magnitude, in increasing values, on the x-axis and mass on the y-axis. The colour corresponds to the z value with yellow being maximum and dark blue being minimum.

When there is no spin there is no 3-dimensional motion since the orbits are initialised within the x-y plane. We see that around the masses of $10^{10} M_{\odot}$ and $10^{11} M_{\odot}$ is where the triplets achieve maximum 3-dimensional motion. At $10^{12} M_{\odot}$, however, there is none. At this mass, the triplets are so massive that black holes merge almost immediately. At $10^{10} M_{\odot}$ and $10^{11} M_{\odot}$, triplets which have much more predictable outcomes gain an added layer of complexity in their dynamics.

At the smaller mass units ($10^0 M_{\odot}$ – $10^2 M_{\odot}$), the influence of spin is not very apparent but as the systems increase in mass, there is an increase in the maximum z-coordinate achieved by the rotating black hole. This falls within the mass range of $10^4 M_{\odot}$ – $10^{10} M_{\odot}$. As the mass unit increases beyond this, there is still 3-dimensional motion but much less than the intermediary masses.

We observe maximum z-motion in the intermediate masses in the non-hierarchical triangles than in the hierarchical triangles. We see this from Fig. 8 where the 3,4,5 on the left represents the non-hierarchical triangles and on the right, the 13,84,85 represents the hierarchical triangles. It is interesting that for the hierarchical triangles, at the larger masses ($10^8 M_{\odot}$ and higher) is where we observe maximum z-motion before swift mergers and end of lifetimes. It is also more noticeable

in the hierarchical triangles than the non-hierarchical triangles that as the spin magnitude increases, the maximum z-coordinate also increases. The major difference between these two types of configurations is the magnitude of the z-values achieved by the rotating black hole. For the non-hierarchical triangles, this is an order of magnitude greater than the hierarchical triangles.

These differences are typical because non-hierarchical configurations are generally more chaotic and unpredictable than hierarchical ones (Anosova et al., 1990; Anosova and Orlov, 1992). In all triangles at the extreme mass unit of $10^{12} M_{\odot}$, systems end almost immediately without enough time to develop motion in the z-axis. These are the blue bands that appear in Figs. 7 and 8.

4. Discussion and conclusion

After an initial study on black hole triplets in Chitan et al. (2021), we wanted to add another level of complexity to the problem by introducing spin. This is one step in making our black hole triplet simulations closer to a realistic black hole triplet. We conducted two main sets of simulations. In the first set we followed the Agekian–Anosova phase space set up. Here we focused only on simulations with zero spin and then simulations with maximum spin. The masses of our triplets stayed fixed at $10^6 M_{\odot}$, with the rotating black hole having a mass of $10 \times 10^6 M_{\odot}$.

From this set one simulations our main takeaway was that adding spin can greatly increase the lifetimes of our black hole triplets, sometimes by several orders of magnitude (Fig. 3). We observed that there was a defined region of the Agekian–Anosova region where the lifetimes of triplets changed significantly with the addition of spin. This region favoured a more non-hierarchical setup of triplets which makes sense since we know that non-hierarchical triplets are more sensitive to changes in initial conditions than the hierarchical triplets.

From set one, 12.9% of our simulations had an actual change in their final outcome when spin was added (Fig. 4). This meant that a

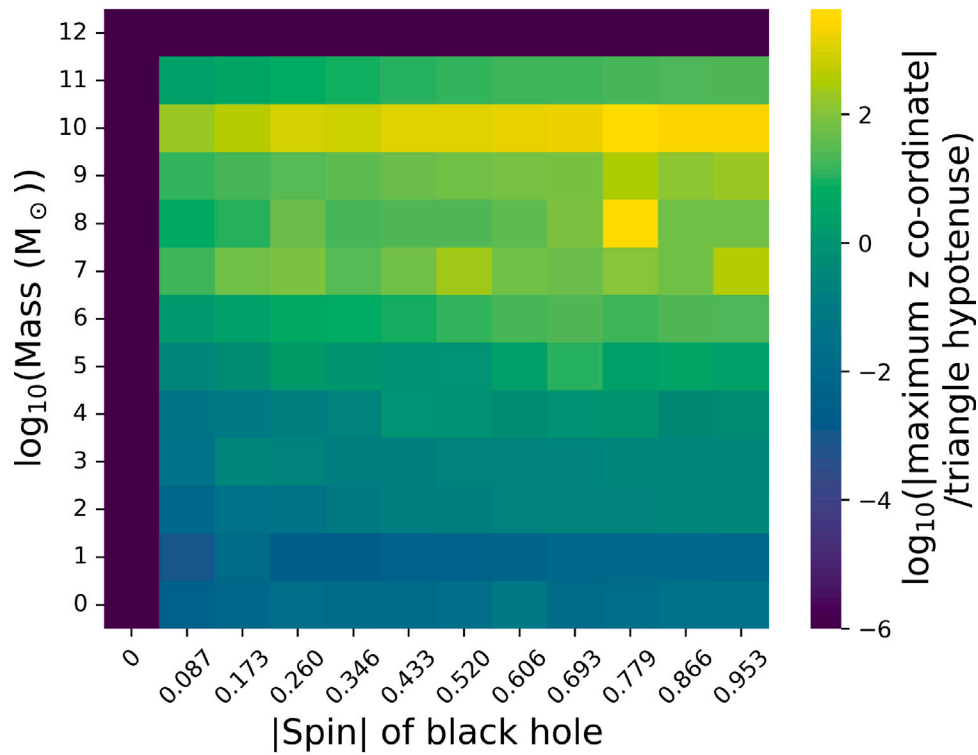


Fig. 7. A colour plot showing a measure of 3-dimensional motion for our triplets of set two. We show the average maximum z-coordinate normalised by the hypotenuse of the corresponding triangle as a function of spin and mass values”.

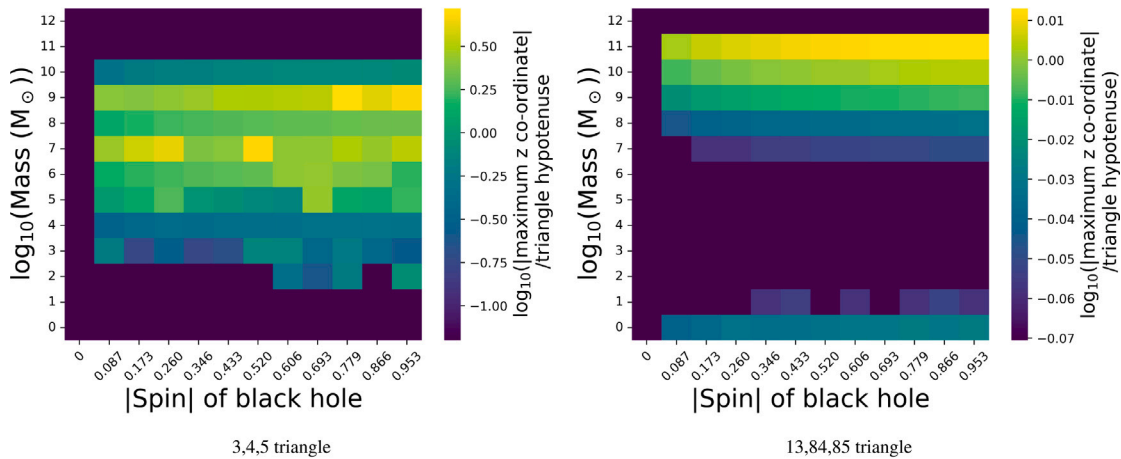


Fig. 8. Colour plots showing a measure of 3-dimensional motion for the 3,4,5 triangle (left) and 13,84,85 (right) triangle of set two. We show the average maximum z-coordinate normalised by the hypotenuse of the corresponding triangle as a function of spin and mass values.

black hole triplet changed the way it ended its life as a triplet. We defined this ‘end of life’ as either being when one black hole escapes the system or when two of the black holes merge with each other. Though > 87% of our triplets did not change their final outcome, there was still some measurable effect of the addition of spin with the lifetimes. When we observe these real-life triplets, this sensitivity should be considered. This is especially so if we try to predict mergers or escapes of supermassive black holes that are part of triplets.

Building on the first set of simulations, we conducted a second set of simulations that we using the set up of Pythagorean triangles. These set two simulations focused on how increasing the spin magnitude would affect our triplets at different masses. In this way, we had 12 different spin magnitudes to test (ranging from 0–0.95) and 13 different masses to look at (ranging from $10^0 M_{\odot}$ to $10^{12} M_{\odot}$). Our main findings from this set of simulations was that it appears that spin has the

greatest effect on black hole triplets at the intermediate mass ranges, particularly for triplets in the mass range of $10^4 M_{\odot}$ – $10^5 M_{\odot}$, and mostly at $10^{4.4} M_{\odot}$. This is based off of the greatest influence of spin on the lifetimes of the black hole triplets. We also considered the effect on the mergers to see if they would be either hindered or promoted with this added spin. We found that at the mass ranges of $10^{4.4} M_{\odot}$ and $10^{5.5} M_{\odot}$, the overall fraction of mergers in our Pythagorean ensemble did not show any significant trends when we increased the spin magnitude.

Our intermediate mass black holes are the most affected because they fulfil two important criteria: they have large enough masses for substantive triplet interaction (compared to low mass black holes that quickly end in escape) and they are small enough that they live for a while before mergers (compared to the large mass black holes). Since they interact more strongly over long time periods, the effect of added spin is more evident. It is important to note that these findings are

restricted to the distance unit fixed at 1 parsec (206265 AU) within our simulations.

In addition to examining the effects of spin magnitude and mass, we also considered the motion in the z -axis in our set two simulations. Specifically, we wanted to determine how much 3-dimensional motion was present. Since our added spin was not perpendicular to the x - y plane, we naturally expected our black holes to become 3-dimensional. Valtonen and Karttunen (2006) showed that when the initial velocities were kept to zero, the movement of the triplets was restricted to the plane. They derived statistical distributions from numerical orbital calculations of the binary energy within a triplet system for both the three-dimensional case and the planar case. They showed that the 2-dimensional case and the 3-dimensional case were statistically different — affecting lifetimes and outcomes of triplets. Here, from our results (Figs. 7), this is corroborated as the inclusion of spin of one of the black holes results in 3-dimensional motion. We found the black hole triplets with mass of $10^{10} M_{\odot}$ to have the largest z -coordinates. This makes the triplets more complex and their behaviour even more chaotic and unpredictable.

In the real astrophysical context, the effect of spin in binary systems has been studied extensively. Stella and Possenti (2009) looked at binary systems of compact objects and the astrophysical environments around these compact systems. The surrounding accretion discs of black holes and neutron stars should be affected by the strong gravity and potentially the Lense-Thirring effect of these rotating bodies. The Lense-Thirring effect refers to the small perturbations induced on the orbit of a test particle around a massive, rotating body (Lense and Thirring, 1918). These effects should be large and noticeable when looking at X-ray flares from the hot accretion discs. The Lense-Thirring effect then could potentially be used to determine certain characteristics about host compact objects.

Valtonen et al. (2010) studied in great detail the OJ287 system, a binary blazar. They concluded that the spin of the primary SMBH of the OJ287 system must influence the orbit of the secondary black hole around it. Using this, they were able to estimate what the spin of the primary SMBH should be. They later observed the flares from this system and were able to conclude that the spin is 0.313 (Valtonen et al., 2016b). The effect of spin on the perihelion precession of the OJ287 system was also studied analytically by Marin and Poveda (2021) and Martinez (2023b). Here they tried to match the amount of perihelion precession obtained theoretically to the observational data by considering the effect of spin. Martinez (2023b) was able to match closely both theoretical and observational perihelion precession for both the OJ287 system as well as the Sagittarius A*-S2 system. Previously, using only a Schwarzschild prescription (Martinez, 2023a), their theoretical predictions did not align with the observational evidence, indicating a need to include the effect of spin in binary black hole models.

Binary systems tend to be less complicated than triplet systems. Tracing the orbits and predicting the spin based on frame-dragging effects are difficult, but feasible for binaries. For the triplet system, these effects, especially on the more non-hierarchical triangles appear to be greatly chaotic and unpredictable. The overall effect of the rotating black hole appears negligible when considering the final states of these systems i.e. mergers and two-body encounters. But, utilising the orbits of these bodies and the potentially observable Lense-Thirring effect on the other two bodies of these types of systems to obtain information about the spin magnitude of a black hole may be quite difficult. The system may not be constrained to the orbital plane which may contribute to unpredictable outcomes.

For triplets of SMBHs, which are expected to form hierarchically via galactic mergers (Valtonen, 1996; Volonteri, 2010; Amaro-Seoane et al., 2010), unpredictability can potentially be limited due to mass being the dominant factor, as we see from this study. Real-life SMBH triplets would tend to form in hierarchical setups and our simulations of hierarchical triangles show that mergers happen much more quickly

than the non-hierarchical triangles and therefore behave less chaotically. Koehn et al. (2023) also looked at SMBH triplets coming from the cosmological simulation, ROMULUS. The heaviest two SMBHs in their simulations always merged on a timescale shorter than Hubble time.

In our study, we included black holes of masses $1 M_{\odot}$ – $3 M_{\odot}$ which are considered to be highly theoretical. There have been a few candidates for the smallest black hole discovered. One of these was found by Lam et al. (2022) via gravitational lensing, where the object could either be the smallest black hole found yet or a neutron star of mass $1.6 - 4.4 M_{\odot}$. When Sahu et al. (2022) observed this object, however, they estimated a mass of around $7 M_{\odot}$. Lam and Lu (2023) re-analysed this object and found that it is closer to $6 M_{\odot}$. Raidal et al. (2019) also studied primordial black holes in the mass range of $0.1 M_{\odot}$ – $10^3 M_{\odot}$ and their merger rates for potential LIGO detections. In some cases they found that a single primordial black hole nearby the binary would be the main disruption of a merger event. Here we find for the most part, small mass triplet systems end in escape over merger with a remnant binary pair which would go on to merge with each other.

Data statement

The data underlying this paper is available at <https://doi.org/10.6084/m9.figshare.19735960.v2>

Code by Prof. Mikkola is available at - <http://www.astro.utu.fi/mikkola/>

Additional code by authors can be found here - <https://doi.org/10.6084/m9.figshare.13194146.v1>

CRediT authorship contribution statement

A. Chitan: Writing – original draft, Methodology, Formal analysis, Conceptualization. **A. Mylläri:** Writing – review & editing, Supervision, Conceptualization. **M. Valtonen:** Writing – review & editing, Supervision, Conceptualization.

Declaration of competing interest

The authors declare that they have no known competing financial interests or personal relationships that could have appeared to influence the work reported in this paper.

Appendix. Agekian-Anosova region extended

To fully cover all the possible geometrical configurations, we also conduct simulations with spinning black hole first, initialised at $(-0.5, 0)$, Run Three, and then initialised at $(0.5, 0)$, Run Four. In both cases, the masses of all the bodies remain as previously described and the spin magnitude on the spinning black hole also is kept at the same value.

For the case where the spinning black hole is kept fixed on the negative axis, the $\log_{10}(\text{lifetime}/\text{crossing time})$ looks like Fig. A.9. The results in this case appear much different than in the other cases as most of the simulations are longer living. This is most likely due to the positioning of the most massive, rotating hole further away from the other two black holes as compared to the previous cases.

In the scenario where the spinning black hole is kept fixed on the positive axis, the $\log_{10}(\text{lifetime}/\text{crossing time})$ of the systems appear Fig. A.10. Longer living systems cluster to the top left — away from the more massive rotating black hole, while systems that start off closer to it (bottom right) end very quickly.

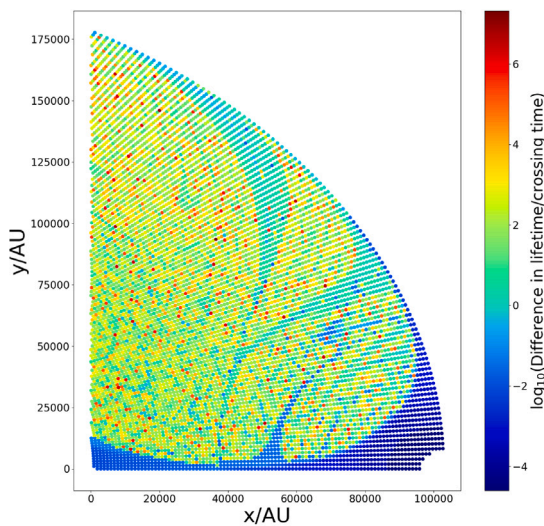


Fig. A.9. The $\log_{10}(\text{lifetime}/\text{crossing time})$ for simulations in the Agekian Anosova region for run three of set one simulations. See Table 1.

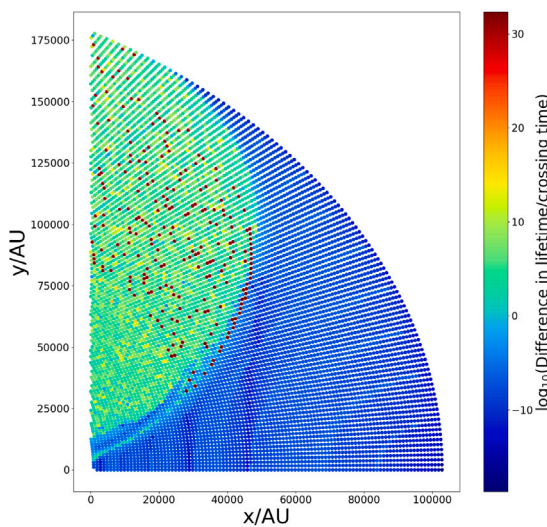


Fig. A.10. The $\log_{10}(\text{lifetime}/\text{crossing time})$ for simulations in the Agekian Anosova region for Run Four of set one simulations. See Table 1.

Data availability

The data underlying this paper is available at <https://doi.org/10.6084/m9.figshare.19735960.v2> (Chitan et al., 2023).

Code by Prof. Mikkola is available at - <http://www.astro.utu.fi/mikkola/>

Additional code by authors can be found here - <https://doi.org/10.6084/m9.figshare.13194146.v1>.

References

- Abbott, B., Abbott, R., Abbott, T., Abraham, S., Acernese, F., Ackley, K., Adams, C., Adhikari, R., Adya, V., Affeldt, C., Agathos, M., Agatsuma, K., Aggarwal, N., Aguiar, O., Aiello, L., Ain, A., Ajith, P., Allen, G., Allocca, A., Aloy, M., et al., 2019. GWTC-1: A gravitational-wave transient catalog of compact binary mergers observed by LIGO and Virgo during the first and second observing runs. *Phys. Rev. X* 9, 031040, <https://link.aps.org/doi/10.1103/PhysRevX.9.031040>.
- Abbott, R., Abbott, T., Abraham, S., Acernese, F., Ackley, K., Adams, A., Adams, C., Adhikari, R., Adya, V., Affeldt, C., Agathos, M., Agatsuma, K., Aggarwal, N., Aguiar, O., Aiello, L., Ain, A., Ajith, P., Akcay, S., Allen, G., Allocca, A., et al., 2021. GWTC-2: Compact binary coalescences observed by LIGO and Virgo

- during the first half of the third observing run. *Phys. Rev. X* 11, 021053, <https://link.aps.org/doi/10.1103/PhysRevX.11.021053>.
- Amaro-Seoane, P., Sesana, A., Hoffman, L., Benacquista, M., Eichhorn, C., Makino, J., Spurzem, R., 2010. Triplets of supermassive black holes: astrophysics, gravitational waves and detection. *Mon. Not. R. Astron. Soc.* 402, 2308–2320.
- Anosova, Z., Nebukin, A., 1991. On the representativity of initial conditions of triple systems. *Astron. Astrophys.* 252, 410–413.
- Anosova, Z., Orlov, V., 1984. The initial configuration and the escape of triple systems with components of different masses. *Tr. Astron. Obs. Leningr.* 39, 101–111.
- Anosova, Z., Orlov, V., 1992. The types of motion in hierarchical and non-hierarchical triple systems - Numerical experiments. *Astron. Astrophys.* 260, 473–484.
- Anosova, J., Orlov, V., Aarseth, S., 1994. Initial conditions and dynamics of triple systems. *Celest. Mech. Dyn. Astron.* 60, 365–372.
- Anosova, J., Orlov, V., Chernin, A., Ivanov, A., Kiseleva, L., 1990. Dynamics and configurations of galaxy triplets. *Int. Astron. Union Colloq.* 124, 633–643. doi:10.1017/s0252921100005765.
- Bardeen, J., Carter, B., Hawking, S., 1973. The four laws of black hole mechanics. *Commun. Math. Phys.* 31, 161–170.
- Barker, B., O'Connell, R., 1975. Gravitational two-body problem with arbitrary masses, spins, and quadrupole moments. *Phys. Rev. D* 12, 329–335. doi:10.1103/physrevd.12.329.
- Belczynski, K., Kalogera, V., Bulik, T., 2002. A comprehensive study of binary compact objects as gravitational wave sources: Evolutionary channels, rates, and physical properties. *Astrophys. J.* 572, 407–431.
- Boekholt, T., Moerman, A., Portegies Zwart, S., 2021. Relativistic Pythagorean three-body problem. *Phys. Rev. D* 104, 083020, <https://link.aps.org/doi/10.1103/PhysRevD.104.083020>.
- Burrau, C., 1913. Numerische Berechnung eines Spezialfalles des Dreikörperproblems. *Astron. Nachr.* 195, 113–118. doi:10.1002/asna.19131950602.
- Chitan, A., Mylläri, A., Haque, S., 2021. Relativistic effects on triple black holes: Burrau's problem revisited. *Mon. Not. R. Astron. Soc.* 509, 1919–1928. doi:10.1093/mnras/stab3124.
- Chitan, A., Mylläri, A., Valtonen, M., 2023. Relativistic effects on triple black holes II the influence of spin in burrau's problem. pp. 1–3, https://figshare.com/articles/dataset/Relativistic_Effects_on_Triple_Black_Holes_II_The_Influence_of_Spin_in_Burrau_s_Problem_1-3_/19735960.
- Ciufolini, I., Pavlis, E., 2004. A confirmation of the general relativistic prediction of the Lense–Thirring effect. *Nature* 431, 958–960.
- Fang, Y., Chen, X., Huang, Q., 2019. Impact of a spinning supermassive black hole on the orbit and gravitational waves of a nearby compact binary. *Astrophys. J.* 887, 210. doi:10.3847/1538-4357/ab510e.
- Fang, Y., Huang, Q., 2019. Secular evolution of compact binaries revolving around a spinning massive black hole. *Phys. Rev. D* 99, 103005, <https://link.aps.org/doi/10.1103/PhysRevD.99.103005>.
- Fang, Y., Huang, Q., 2020. Three body first post-Newtonian effects on the secular dynamics of a compact binary near a spinning supermassive black hole. *Phys. Rev. D* 102, 104002, <https://link.aps.org/doi/10.1103/PhysRevD.102.104002>.
- Ginat, Y., Perets, H., 2021. Analytical, statistical approximate solution of dissipative and nondissipative binary-single stellar encounters. *Phys. Rev. X* 11, e031020.
- Goodman, J., Hut, P., 1993. Binary–single-star scattering. V. Steady state binary distribution in a homogeneous static background of single stars. *Astrophys. J.* 403, 271.
- Hamers, A., Samsing, J., 2019. Analytic computation of the secular effects of encounters on a binary: features arising from second-order perturbation theory. *Mon. Not. R. Astron. Soc.* 487, 5630–5648.
- Hawking, S., 1972. Black holes in general relativity. *Commun. Math. Phys.* 25, 152–166.
- Heggie, D., Hut, P., 1993. Binary–single-star scattering. IV. Analytic approximations and fitting formulae for cross sections and reaction rates. *Astrophys. J.* 85, 347.
- Heggie, D., Hut, P., McMillan, S., 1996. Binary–single-star scattering. VII. Hard binary exchange cross sections for arbitrary mass ratios: Numerical results and semianalytic FITS. *Astrophys. J.* 467, 359.
- Heggie, D., Rasio, F., 1996. The effect of encounters on the eccentricity of binaries in clusters. *Mon. Not. R. Astron. Soc.* 282, 1064–1084.
- Hellström, C., Mikkola, S., 2010. Explicit algorithmic regularization in the few-body problem for velocity-dependent perturbations. *Celest. Mech. Dyn. Astron.* 106, 143–156. doi:10.1007/s10569-009-9248-8.
- Hoffman, L., Loeb, A., 2007. Dynamics of triple black hole systems in hierarchically merging massive galaxies. *Mon. Not. R. Astron. Soc.* 377, 957–976. doi:10.1111/j.1365-2966.2007.11694.x.
- Hut, P., 1983. Binary-single star scattering. II - Analytic approximations for high velocity. *Astrophys. J.* 268, 342–355.
- Hut, P., 1993. Binary–single-star scattering. III. Numerical experiments for equal-mass hard binaries. *Astrophys. J.* 403, 256.
- Hut, P., Bahcall, J., 1983. Binary-single star scattering. I - Numerical experiments for equal masses. *Astrophys. J.* 268, 319–341.
- Israel, W., 1967. Event horizons in static vacuum space-times. *Phys. Rev.* 164, 1776–1779.
- Israel, W., 1968. Event horizons in static electrovac space-times. *Commun. Math. Phys.* 8, 245–260.

- Kerr, R., 1963. Gravitational field of a spinning mass as an example of algebraically special metrics. *Phys. Rev. Lett.* 11, 237–238. <https://link.aps.org/doi/10.1103/PhysRevLett.11.237>.
- Kidder, L., 1995. Coalescing binary systems of compact objects to (post)^{5/2}-Newtonian order. V. Spin effects. *Phys. Rev. D* 52, 821–847. <https://link.aps.org/doi/10.1103/PhysRevD.52.821>.
- Koehn, H., Just, A., Berczik, P., Tremmel, M., 2023. Dynamics of supermassive black hole triples in the ROMULUS25 cosmological simulation. *Astron. Astrophys.* 678, eA11.
- Kollatschny, W., Weilbacher, P., Ochmann, M., Chelouche, D., Monreal-Ibero, A., Bacon, R., Contini, T., 2020. NGC 6240: A triple nucleus system in the advanced or final state of merging. *Astron. Astrophys.* 633, A79. doi:10.1051/0004-6361/201936540.
- Kormendy, J., Richstone, D., 1995. Inward bound—The search for supermassive black holes in galactic nuclei. *Annu. Rev. Astron. Astrophys.* 33, 581–624. doi:10.1146/annurev.aa.33.090195.003053.
- Lam, C., Lu, J., 2023. A reanalysis of the isolated black hole candidate OGLE-2011-BLG-0462/MOA-2011-BLG-191. *Astrophys. J.* 955, e116.
- Lam, C., Lu, J., Udalski, A., Bond, I., Bennett, D., Skowron, J., Mróz, P., Poleski, R., Sumi, T., Szymański, M., Kozłowski, S., Pietrukowicz, P., Soszyński, I., Ulaczyk, K., Wyrzykowski, L., Miyazaki, S., Suzuki, D., Koshimoto, N., Rattenbury, N., Hosek, M., Abe, F., Barry, R., Bhattacharya, A., Fukui, A., Fujii, H., Hirao, Y., Itow, Y., Kirikawa, R., Kondo, I., Matsubara, Y., Matsumoto, S., Muraki, Y., Olschenko, G., Ranc, C., Okamura, A., Satoh, Y., Silva, S., Toda, T., Tristram, P., Vandenbergh, A., Yama, H., Abrams, N., Agarwal, S., Rose, S., Terry, S., 2022. An isolated mass-gap black hole or neutron star detected with astrometric microlensing. *Astrophys. J.* 933, eL23.
- Lense, J., Thirring, H., 1918. Über den Einfluß der Eigenrotation der Zentralkörper auf die Bewegung der Planeten und Monde nach der Einsteinschen Gravitationstheorie. *Phys. Z.* 19, 156.
- Marin, C., Poveda, J., 2021. Spin contribution to the perihelion advance in binary systems like OJ 287: higher order corrections. *Astrophys. Space Sci.* 366, e107.
- Martinez, D., 2023a. Alternate method of correction to the perihelion precession of binary systems. *Astrophys. Space Sci.* 368, e36.
- Martinez, D., 2023b. Spin contributions to the alternate correction to the perihelion precession of binary systems such as OJ287. *Astrophys. Space Sci.* 368, e45.
- McMillan, S., Hut, P., 1996. Binary–single-star scattering. VI. Automatic determination of interaction cross sections. *Astrophys. J.* 467, 348.
- McMillan, S., Portegies Zwart, S., 2001. Black hole mergers in the universe. *Dyn. Star Clust. Milky Way* 228, 517.
- Mikkola, S., 2020a. Motion in the field of a black hole. In: *Gravitational Few-Body Dynamics*. pp. 211–220. doi:10.1017/9781108868105.011.
- Mikkola, S., 2020b. Motion in the field of a black hole. In: *Gravitational Few-Body Dynamics*. pp. 211–220. doi:10.1017/9781108868105.011.
- Mikkola, S., Aarseth, S., 1993. An implementation of N-body chain regularization. *Celest. Mech. Dyn. Astron.* 57, 439–459. doi:10.1007/bf00695714.
- Mikkola, S., Aarseth, S., 1996. A slow-down treatment for close binaries. *Celest. Mech. Dyn. Astron.* 64, 197–208. doi:10.1007/bf00728347.
- Mikkola, S., Aarseth, S., 2002. A time-transformed leapfrog scheme. *Celest. Mech. Dyn. Astron.* 84, 343–354.
- Mikkola, S., Merritt, D., 2006. Algorithmic regularization with velocity-dependent forces. *Mon. Not. R. Astron. Soc.* 372, 219–223. doi:10.1111/j.1365-2966.2006.10854.x.
- Mikkola, S., Merritt, D., 2008. Implementing few-body algorithmic regularization with post-Newtonian terms. *Astron. J.* 135, 2398–2405. doi:10.1088/0004-6256/135/6/2398.
- Mikkola, S., Tanikawa, K., 1999. Explicit symplectic algorithms for time-transformed Hamiltonians. *Celest. Mech. Dyn. Astron.* Vol. 74, 287–295.
- Mikkola, S., Tanikawa, K., 2013a. Implementation of an efficient logarithmic-Hamiltonian three-body code. *New Astron.* 20, 38–41. doi:10.1016/j.newast.2012.09.004.
- Mikkola, S., Tanikawa, K., 2013b. Regularizing dynamical problems with the symplectic logarithmic Hamiltonian leapfrog. *Mon. Not. R. Astron. Soc.* 430, 2822–2827. doi:10.1093/mnras/stt085.
- Monaghan, J., 1976. A statistical theory of the disruption of three-body systems - I. Low angular momentum. *Mon. Not. R. Astron. Soc.* 176, 63–72.
- Mora, T., Will, C., 2004. Post-Newtonian diagnostic of quasioequilibrium binary configurations of compact objects. *Phys. Rev. D* 69, 104021. <https://link.aps.org/doi/10.1103/PhysRevD.69.104021>.
- Peetre, J., 1995. Outline of a scientific biography of Ernst Meissel (1826–1895). *Hist. Math.* 22, 154–178. doi:10.1006/hmat.1995.1015.
- Peifker, F., Zajaček, M., Labaj, M., Thomkins, L., Elbe, A., Eckart, A., Labadie, L., Karas, V., Sabha, N., Steiniger, L., Melamed, M., 2024. The evaporating massive embedded stellar cluster IRS 13 close to Sgr A*. II. Kinematic structure. *Astrophys. J.* 970, e74.
- Raidal, M., Spethmann, C., Vaskonen, V., Veermäe, H., 2019. Formation and evolution of primordial black hole binaries in the early universe. *J. Cosmol. Astropart. Phys.* 2019, 018. doi:10.1088/1475-7516/2019/02/018.
- Rhoads, K., Wyithe, J., 2005. Realistic event rates for detection of supermassive black hole coalescence by LISA. *Mon. Not. R. Astron. Soc.* 361, 1145–1152. doi:10.1111/j.1365-2966.2005.08987.x.
- Rodriguez, C., Antonini, F., 2018. A triple origin for the heavy and low-spin binary black holes detected by LIGO/VIRGO. *Astrophys. J.* 863, 7. doi:10.3847/1538-4357/aace44.
- Sahu, K., Anderson, J., Casertano, S., Bond, H., Udalski, A., Dominik, M., Calamida, A., Bellini, A., Brown, T., Rejkuba, M., Bajaj, V., Kains, N., Ferguson, H., Fryer, C., Yock, P., Mróz, P., Kozłowski, S., Pietrukowicz, P., Poleski, R., Skowron, J., Soszyński, I., Szymański, M., Ulaczyk, K., Wyrzykowski, L., Barry, R., Bennett, D., Bond, I., Hirao, Y., Silva, S., Kondo, I., Koshimoto, N., Ranc, C., Rattenbury, N., Sumi, T., Suzuki, D., Tristram, P., Vandenbergh, A., Beaulieu, J., Marquette, J., Cole, A., Fouqué, P., Hill, K., Dieters, S., Coutures, C., Dominis-Prester, D., Bennett, C., Bachelet, E., Menzies, J., Albrow, M., Pollard, K., Gould, A., Yee, J., Allen, W., Almeida, L., Christie, G., Drummond, J., Gal-Yam, A., Gorbikov, E., Jablonski, F., Lee, C., Mao, Z., Manulis, I., McCormick, J., Natusch, T., Pogge, R., Shvartzvald, Y., Jørgensen, U., Alsubai, K., Andersen, M., Bozza, V., Novati, S., Burgdorf, M., Hinse, T., Hundertmark, M., Husser, T., Kerins, E., Longa-Peña, P., Mancini, L., Penny, M., Rahvar, S., Ricci, D., Sajadian, S., Skottfelt, J., Snodgrass, C., Southworth, J., Tregloan-Reed, J., Wambsgans, J., Wertz, O., Tsapras, Y., Street, R., Bramich, D., Horne, K., Steele, I., RoboNet Collaboration, 2022. An isolated stellar-mass black hole detected through astrometric microlensing. *Astrophys. J.* 933, e83.
- Sigurdsson, S., Hernquist, L., 1993. Primordial black holes in globular clusters. *Nature* 364, 423–425.
- Stella, L., Possenti, A., 2009. Lense-thirring precession in the astrophysical context. *Space Sci. Rev.* 148, 105–121. doi:10.1007/s11214-009-9627-1.
- Stone, N., Leigh, N., 2019. A statistical solution to the chaotic, non-hierarchical three-body problem. *Nature* 576, 406–410.
- Szebehely, V., Peters, C., 1967. Complete solution of a general problem of three bodies. *Astron. J.* 72, 876. doi:10.1086/110355.
- Valtonen, M., 1996. Triple black hole systems formed in mergers of galaxies. *Mon. Not. R. Astron. Soc.* 278, 186–190. doi:10.1093/mnras/278.1.186.
- Valtonen, M., Anosova, J., Kholshevnikov, K., Mylläri, A., Orlov, V., Tanikawa, K., 2016a. From comets to chaos. In: *The Three-Body Problem from Pythagoras to Hawking*. pp. 51–84.
- Valtonen, M., Karttunen, H., 2006. *The Three-Body Problem*. Cambridge University Press.
- Valtonen, M., Mikkola, S., Merritt, D., Gopakumar, A., Lehto, H., Hyvönen, T., Rampadarath, H., Saunders, R., Basta, M., Hudec, R., 2010. Measuring the spin of the primary black hole in oJ287. *Astrophys. J.* 709, 725–732. doi:10.1088/0004-637x/709/2/725.
- Valtonen, M., Mikkola, S., Pietila, H., 1995. Burrau's three-body problem in the post-Newtonian approximation. *Mon. Not. R. Astron. Soc.* 273, 751–754.
- Valtonen, M., Zola, S., Ciprini, S., Gopakumar, A., Matsumoto, K., Sadakane, K., Kidger, M., Gazeas, K., Nilsson, K., Berdyugin, A., Pirola, V., Jermak, H., Baliyan, K., Alicavus, F., Boyd, D., Campas Torrent, M., Campos, F., Carrillo Gómez, J., Caton, D., Chavushyan, V., Dalessio, J., Debski, B., Dimitrov, D., Drozd, M., Er, H., Erdem, A., Escartín Pérez, A., Fallah Ramazani, V., Filippenko, A., Ganesh, S., Garcia, F., Gómez Pinilla, F., Gopinathan, M., Haislip, J., Hudec, R., Hurst, G., Ivarsen, K., Jelínek, M., Joshi, A., Kagitani, M., Kaur, N., Keel, W., LaCluyze, A., Lee, B., Lindfors, E., Lozano de Haro, J., Moore, J., Mugrauer, M., Naves Noguez, R., Neely, A., Nelson, R., Ogloza, W., Okano, S., Pandey, J., Perri, M., Pihajoki, P., Poyner, G., Provencal, J., Pursimo, T., Raj, A., Reichart, D., Reinthal, R., Sadeghi, S., Sakanoi, T., Salto González, J., Sameer Schweyer, T., Siwak, M., Soldán Alfaro, F., Sonbas, E., Steele, I., Stocke, J., Strobl, J., Takalo, L., Tomov, T., Tremosa Espasa, L., Valdes, J., Valero Pérez, J., Verrecchia, F., Webb, J., Yoneda, M., Zejmo, M., Zheng, W., Telting, J., Saario, J., Reynolds, T., Kvammen, A., Gafton, E., Karjalainen, R., Harmanen, J., Blay, P., 2016b. Primary black hole spin in OJ 287 as determined by the general relativity centenary flare. *Astrophys. J.* 819, eL37.
- Vigna-Gómez, A., Toonen, S., Ramirez-Ruiz, E., Leigh, N., Riley, J., Haster, C., 2021. Massive stellar triples leading to sequential binary black hole mergers in the field. *Astrophys. J.* 907, L19. doi:10.3847/2041-8213/abd5b7.
- Vitral, Eduardo, Mamon, Gary A., 2021. Does NGC 6397 contain an intermediate-mass black hole or a more diffuse inner subcluster? *Astron. Astrophys.* 646, A63. doi:10.1051/0004-6361/202039650.
- Volonteri, M., 2010. Formation of supermassive black holes. *Astron. Astrophys. Rev.* 18, 279–315.
- Wald, R., 1999. Gravitational collapse and cosmic censorship. In: *Black Holes, Gravitational Radiation and the Universe: Essays in Honor of C.V. Vishveshwara*. pp. 69–86. doi:10.1007/978-94-017-0934-7.5.
- Will, C., 2014a. Incorporating post-Newtonian effects in N-body dynamics. *Phys. Rev. D* 89, doi:10.1103/physrevd.89.044043.
- Will, C., 2014b. Post-Newtonian effects in N-body dynamics: conserved quantities in hierarchical triple systems. *Class. Quantum Gravity* 31, 244001. doi:10.1088/0264-9381/31/24/244001.
- Yadav, Jyoti, Das, Mousumi, Barway, Sudhanshu, Combes, Françoise, 2021. A triple active galactic nucleus in the NGC 7733-7734 merging group. *Astron. Astrophys.* 651, L9. doi:10.1051/0004-6361/202141210.